Journal of New Materials for Electrochemical Systems 17, 219-224 (2014)

In-Situ Preparation of Si@C Composite Anode Materials for Lithium Ion Batteries

Qingwei Cui[1,2], Jiang Cao[1], Mou Fang[1], Jianjun Li[1],Fang Lian[2],Li Wang[1,4,†], Xiangming He[1,3,*]

[1]Institute of Nuclear and New Energy Technology,Tsinghua University, Beijing 100084, PR China
[2]School of Materials Science and Engineering, University of Science and Technology Beijing, Beijing 100083, PR China
[3]State Key Laboratory of Automotive Safety and Energy, Tsinghua University, Beijing 100084, PR China
[4]Beijing Key Lab of Fine Ceramics, Tsinghua University, Beijing 100084,PR China

Received: December 10, 2013, Accepted: September 26, 2014, Available online: November 26, 2014

Abstract: *A Si@C nanocomposite material is prepared via in-situ polymerization of acrylonitrile on the surface of silicon nanoparticles, and followed by carbonization in an inert atmosphere. The obtained Si@C nanocomposite material is composed of a nanosized Si core and a casting carbon shell. Its structure and electrochemical properties are characterized by XRD, TG, Raman, SEM, TEM and charge-discharge performance test. The results obtained in this study show that Si@C nanocomposite is coated by a layer of amorphous carbon which provides a conductive matrix and relieves the dramatically morphological changes of Si upon lithium insertion and extraction. The composite exhibits good capacity retention for use as anode in lithium-ion batteries. This study also paves a facile and industrial scalable way to prepare core/shell structure for high performance anode materials for lithium-ion batteries.*

Keywords: in-situ; polymerization; silicon-carbon composite; anode material; lithium-ion battery

1. INTRODUCTION

Environmental friendly and rechargeable lithium-ion batteries are significant to the development of portable electronic devices, electric vehicles (EV) and electric and hybrid vehicles (EHV). Due to the rapid development of such equipment there is an increasing demand for lithium-ion batteries with high energy densities and good cycleability [1-5]. As a traditional anode material, graphite can't meet with those requirements owing to its limited theoretical specific capacity (~372mAh g^{-1}) [6-8]. Tremendous efforts have been made to improve the capacity and thermal stability of new alternative anode materials in the past decade, such as metal oxides [9,10], Sn-based composites [11-13], Si-based composites [14-17] and carbon-alloy composites [18]. Silicon, as one of the most promising candidates for anode materials, has attracted many researchers' attention, primarily due to its numerous appealing advantages: in terms of the highest theoretical capacity ($Li_{4.4}Si$≈4200 mAh g^{-1}) among all known materials, relatively low discharge potential (~0.5V versus Li^+/Li), natural abundance, safety and environmental benignity [19-23].

Unfortunately, Si-based anodes still face two major obstacles: low intrinsic electric conductivity and sever volume changes (~400%) during charging and discharging process, which result in fracture, loss of electric contact and a continuous growth of unstable solid electrolyte interphase (SEI) on the surface [24-25]. Recently, encouraging progresses have been achieved by decreasing the particle size [26,27], and nanostructuring of Si, for example: nanowires [28], nanospheres [29], nanotubes [30,31], nanofibers [32], and silicon/carbon composite [33]. Among all of those approaches, silicon/carbon composite attracts great interest because the good electrical conductivity and stress-buffer nature of carbon can improve the cycle stability of Si-based anodes [34]. Methods such as ball milling Si nano-particles and carbon [35], typical dissolving-mixing-pyrolyzing [36], spray-pyrolysis technique [33], chemical vapor deposition (CVD) [37] and thermal vapour deposition (TVD) [38] are employed by many groups to prepare the silicon/carbon composite. However, those methods involve high energy consumption and complex procedures, and it is hard to homogeneously encapsulate the high-surface-energy silicon nanoparticles with uniform carbon layer.

In this study, Si core in carbon shell (Si@C) composite is synthesized via in situ polymerization of acrylonitrile monomer in the surface of nano silicon particles (nano-SPs), followed by carbonization in an inert atmosphere. In detail, the hydroxyl group of the

To whom correspondence should be addressed:
* hexm@tsinghua.edu.cn, Phone: +86 10 89796073, Fax: +86 10 89796031
† wang-l@tsinghua.edu.cn, Phone: +86 10 89796073, Fax: +86 10 89796031

presence of nanocrystalline silicon powder and the silicon hydroxyl of vinyl triethoxy silane under the condition of acid hydrolysis react in a certain temperature making the silicon surface with organic double bond functional group(C=C). Under the effect of benzoyl peroxide, polymer polyacrylonitrile (PAN) by in situ polymerization reaction via the free redicals chemically grafting onto the surface of inorganic silicon particles. After carbonization, the surface of silicon particles is uniformly and closely coated by amorphous carbon layer. On one hand, the presence of amorphous carbon acts as an effectively conductive matrix and prevents the aggregation of silicon nanoparticles. On the other hand, uniform carbon coatings effectively prevents the direct contact of silicon with the electrolyte during cycling, both of which ensure the integrity of the structure and the stability of the interface of electrodes.

2. EXPERIMENTAL

2.1. Material preparation

Preparation of Si@C composite: Firstly, nanocrystalline silicon powder (1.2g, 80-100 nm, Hefei Kaier Nanometer energy & technology Co., Ltd) was dispersed in ethanol solution (100 ml), then hydrofluoric acid(1.5 ml, 40 wt %) was slowly added into the mixture suspension to remove the oxides on the surface of the silicon; after 1 hour, deionized water and ethanol (100ml ,v/v=1:1) was poured to dilute the above solution with the help of ultrasonic by the powerful ultrasonic magnetic cell crusher for 3 hours at room temperature. Subsequently, the hydrolyzing vinyl triethoxy silane (VTES, 1ml, as coupling agent) in nitric acid solution (65 wt%, as catalyst) was dropwised to the mixture solution. After 4 hours, acrylonitrile monomer (AN, 5ml, without inhibitors) and benzoyl peroxide (BPO, 0.05 g, as initiator) was injected into the initial dispersion, then the reaction mixture was mechanically stirred at 80ºC for 12 h in a three mouth flask with nitrogen protection. Then the product obtained was washed and filtered with deionized water and ethanol for 3 times and then dried at 80ºC for 2 hours to yield silicon coated polyacrylonitrile precursor (Si@PAN). The precursor was carbonized under protection of argon at 700ºC for 4 h with the heating rate of 5ºC/min in a tube furnace to obtain the Si@C composite.

For comparison, a Si/C composite was prepared by a traditional mechanical ball-milling method. polyacrylonitrile (PAN, 1.0g) was dissolved in N-methypyrrolidinone (NMP,10ml). Then nanocrystalline silicon powder and PAN solution were subjected to mechanical milling in a high energy ball mill for 3 h with a ball to powder weight ratio of 10:1. After ball milling, the mixture was carbonized under protection of argon at 700ºC for 4 h with the heating rate of 5ºC/min in a tube furnace to obtain the Si/C composite.

2.2. Materials characterization

The obtained Si@C black powders were characterized by powder X-ray diffraction (XRD, Bruker D8 Advance X-ray diffractometer in a Bragg–Brentano configuration) from 10° to 80° with a step size of 0.02°. Thermal gravimetric analysis was performed using Q2000 (TA Instruments) under air atmosphere in temperature range from 30 to 800ºC with a heating rate of 10ºC min^{-1}. Raman spectra were recorded by a Microscopic Confocal Raman Spectrometer (RM2000, Renishaw, England). Field emission scanning electron microscope (FESEM, JEOL JSM-7001F) and transmission electron microscope (TEM, H-800, Hitachi, Japan) were used to study the morphology and microstructure of the Si@C composite.

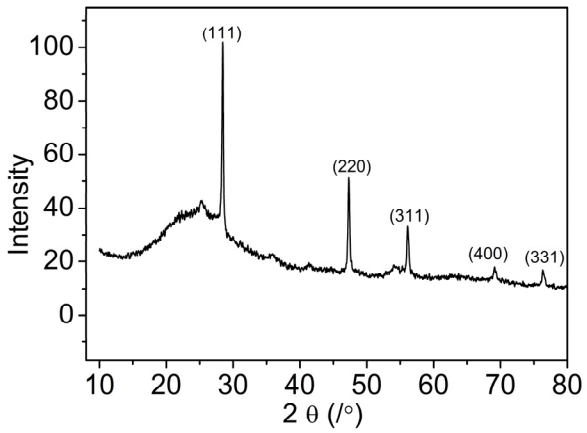

Figure 1. XRD patterns of the as-prepared Si@C composite.

2.3. Electrochemical performance

The electrochemical performances were tested using CR2032 coin-type test cells with lithium foil as the counter and reference electrode. Ethylene carbonate/Diethyl carbonate (EC: DEC=1:1v/v) solution containing 1 mol $LiPF_6$ was used as electrolyte. The porous polypropylene film (Celgard 2400) was used as separator. The working electrode was prepared from a mixture consisting of 70 wt% Si@C composite, 20 wt% acetylene black, and 10 wt% Polytetrafluoroethylene (PTFE, as binder), using ethanol as dispersant. The electrodes were dried at 120ºC under vacuum for 24 h. The half-coin cells were assembled in an argon-filled glove box (M.Braun, Germany) and. The galvanostatic charge-discharge tests were carried out on a Land battery system (Wuhan Kingnuo Electronics Co., Ltd., China) at room temperature with a current density of 50 mA g^{-1}. The cut-off voltage was 0.005 V versus Li/Li^+ for discharge (Li insertion) and 2.0 V versus Li/Li^+ for charge (Li extraction). For comparison, the electrochemical performances of Si/C and pure nanosized Si were evaluated under the same conditions. Electrochemical impedance spectroscopy (EIS) measurements were performed over the frequency range from 100 kHz to 0.1 Hz with ac amplitude of 0.01V on a Solartron 1250 impedance/gain-phase analyzer after 20 cycles and at a stable testing temperature of 25ºC.

3. RESULTS AND DISCUSSION

X-ray diffraction (XRD) and Thermal gravimetric analysis (TG) analysis were conducted to investigate the existence and content of the carbon. The XRD patter of as-prepared Si core carbon shell (Si@C) nanocomposite (Fig. 1) shows sharp diffraction peaks of crystalline Si (JCPDS card 27-1402) corresponding to (111), (220), (311), (400), (331) planes consistent with the paper [39] and a broad peak near 24° which indicates the amorphous feature of the polymer polyacrylonitrile (PAN) pyrolyzed carbon. No other diffraction peaks were observed in the XRD pattern, which means that there is no superfluous miscellaneous phase. Thermal gravimetric analysis (TG) (Fig. 2) shows that the carbon content is 24%, and that indicates that the nature of carbon in the composites is amor-

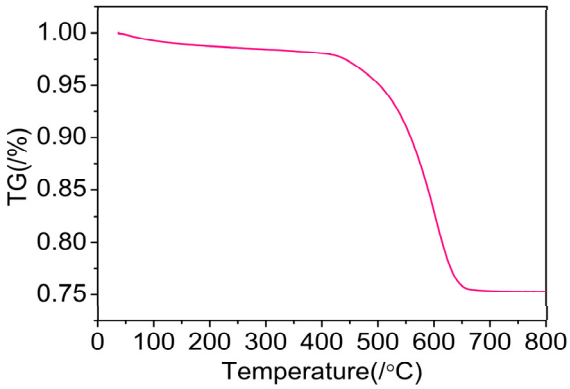

Figure 2. Thermal gravimetric (TG) curve of the as-prepared Si@C composite in air atmosphere.

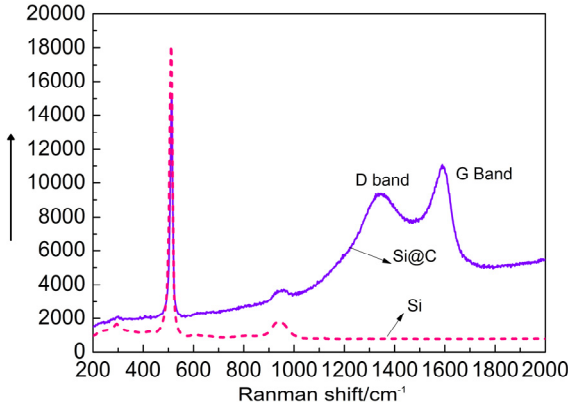

Figure 3. Raman spectra of the silicon nanoparticles before and after carbon coating (solid line: Si@C composite, dotted line: pristine Si).

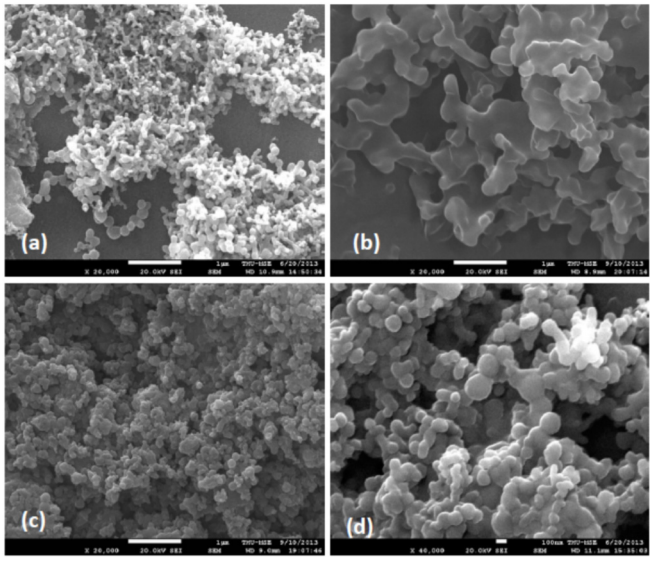

Figure 4. FESEM micrograph of the silicon nanoparticles (SiNPs) polyacrylonitrile coated silicon particles (Si@PAN) and (higher magnification) of the Si@C core/shell nanocomposite.

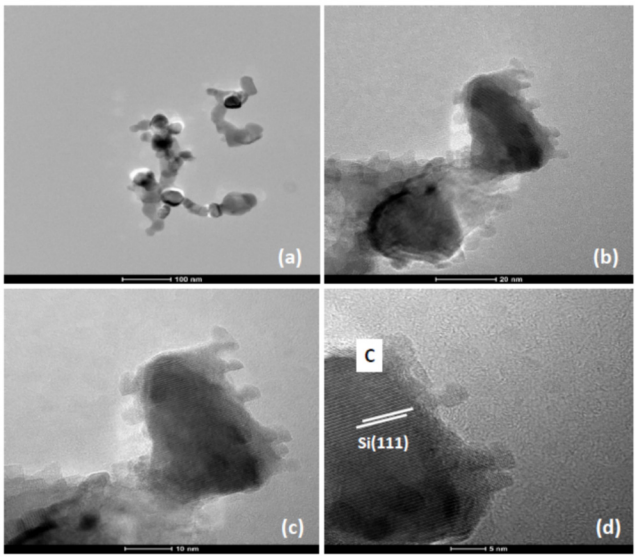

Figure 5. TEM images of the Si@C composite (a, b) and High resolution transmission electron microscopy (HRTEM) (c, d) shows highly crystalline Si core and amorphous carbon shell.

phous. Furthermore, in order to indentify the presence of carbon, the Raman spectra of the pure silicon nanoparticles and the Si@C composite is performed. As shown in Fig. 3, an apparent difference can be observed between the two samples. For Si@C nanocomposites with relative low intensity, the Raman spectra contains the characteristic wide D band and G band around 1340 and 1590 cm^{-1}, respectively, typical for amorphous carbon or disordered graphite, which can also be detected from the following TEM images. In addition, the relatively strong G peak illustrates the carbon is part of graphitization, meaning that carbon layer has better electronic transmission capacity which has an important effect on the followed electrochemical performance [40].

Fig. 4 shows field emission scanning electron microscope microscopy (FESEM) images of the microstructure of the synthesis Si@C nanocomposite. As shows in Fig. 4a, the particle size of nano-silicon is about 80-100 nm. As a result of continues ultrasonic irradiation in the mixed solvent, the nano-silicon particles distributed uniformly.. Typically, silicon coated polyacrylonitrile precursor (Si@PAN) (Fig. 4b) consists of a hierarchical network structure with typical diameters around 100-200 nm. It is clear to see that the surface of silicon nanoparticles are uniformly encapsulated by the organic polymer PAN via in situ free radical polymerization, which is chemical grafted but not physical coated onto the surface of inorganic silicon particles. As the polymer PAN is formed in the presence of the silicon particles, the SiNPs are intimately contacted with the polymer matrix both on the molecular and microscope level. Fig. 4c (lower magnification) and Fig. 4d (higher magnification) show the FESEM images of the as-prepared Si@C nanocomposite. There is a distinct difference between the pristine silicon nanoparticles and the Si@C nanocomposite particles because that the Si@C nanocomposite particles are uniformly and closely encapsulated by amorphous carbon layer after the carbonization of the polymer PAN.

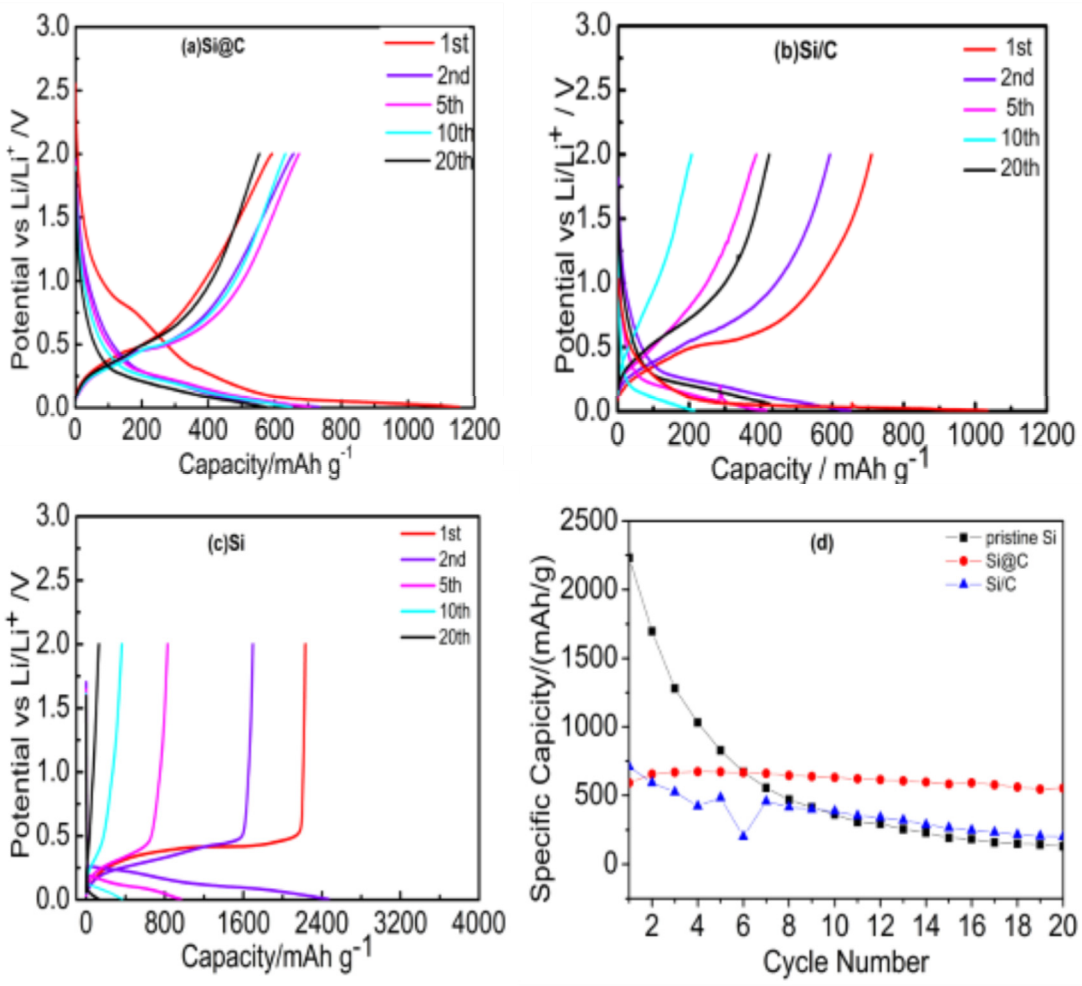

Figure 6. Charge and discharge curves of (a) the Si@C composite, (b) the Si/C composite and (c) pristine Si for the 1st, 2nd, 5th, 10th and 20th cycles, and (d) the cycling performance of pristine Si, Si@C and Si/C.

Fig. 5 shows TEM photographs of uniform spherical nanoparticles of the Si@C composite with an average diameter of 100 nm. High resolution transmission electron microscopy HRTEM **(**Fig. 5 (c, d)**)** shows that these particles have a highly crystalline Si core and half-ordered carbon shell. It is evident to observe that the surface of all silicon nanoparticles (black particles) is coated with a layer of carbon. About 5 nm thickness of the carbon layer forms a complete shell which makes the composite a hetero-generous structure.

The electrochemical performances of the Si@C composite, Si/C composite and pristine Si are tested by galvanostatic charge-discharge tests using coin-type cells at a current density of 50 mAh g^{-1} in the potential range of 0.005-2 V. The specific capacity and current density are based on the active materials weight. Fig. 6 provides voltage profiles of the Si@C composite (a) and the Si/C composite (b) for the 1st, 2nd, 5th, 10th and 20th cycle. As exhibited in Fig. 6a, a long slope in the voltage range of 0.1-0.8 V relates to the formation of solid electrolyte interface (SEI) film, which disappears in the sequent cycles. The initial discharge (Li insertion) and charge (Li extraction) capacities of the Si@C composite are 1196.4 and 633.1 mAh g^{-1}, respectively, and electrochemical reversibility is rapidly enhanced from the 2nd cycle until 10th cycle, and the coulombic efficiency is above 95% after 5 cycles. After 20 cycles, the reversible capacity is 563.2 mAh g^{-1} and the capacity retention is 88.9%. The initial irreversible capacity partly is attributed to the formation of the SEI on the surface, and partly due to the fact that the inner silicon core coated carbon shell takes longer time to active, which can be clearly seen from the increasing charge capacity and coulombic efficiency of the subsequent cycles. The first discharge and charge capacities of the Si/C composite (Fig. 6b), by contrast, are 1034.4 and 710 mAh g^{-1}, respectively, but the reversible capacity rapidly reduced to 193.5 mAh g^{-1} and the capacity retention is merely 27.2% after 20 cycles. The conventional Si/C composite cannot limit the sever volume change of active silicon during cycling and the deviation of Si phase is inevitable [43]. Fig. 6c shows the cycling performance of pristine Si, Si@C and Si/C. It can be observed that pristine Si nanoparticles delivery quite high discharge and charge capacities of about 3645.5 and 2231.2 mAh g^{-1} for the first cycle, respectively. However, after 20 cycles, the reversible capacity rapidly drops to 129.5 mAh g^{-1} with the

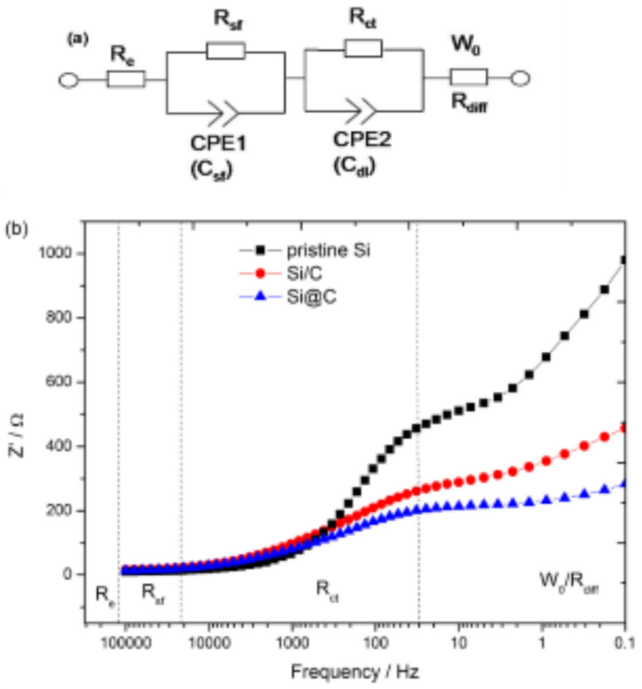

Figure 7. AC impedance spectra of the cells with pristine Si, Si@C and Si/C composite electrodes after 20 cycles: (a) equivalent circuit for the impedance spectra, (b) Z' to Frequency.

capacity retention of only 5.8%. Compared to the above two samples, the Si@C composite shows good cycle stability and capacity retention after 20 cycles.

Thanks to the coexistence of the carbon layer, the direct contact of silicon with the electrolyte during cycling was avoided in some degree, which may prohibit the formation of SEI films on the surface of the Si surface. The improved cycling property of the Si@C composite may be largely attributed to the silicon nanoparticles core in uniform carbon shell structure, which buffers the sever volume change of active silicon during cycling, prevents its fragmentation and pulverization under mechanical stress, and therefore ensures the integrity of the structure and the stability of the interface of electrodes [41].

To further investigate the improved lithium storage performance of Si@C composite in comparison with Si/C composite and pristine Si, electrochemical impedance spectroscopy (EIS) measurements were performed after 20 cycles (frequency range 1 Hz to 100 KHz, at a stable testing temperature of 25ºC). As shown in Fig. 7(b), R_e represents the resistive contribution arising from the electrolyte resistance and the cell components. R_{sf} and C_{sf} (CPE1), which are associated with the high-frequency semicircle, are the SEI film resistance and its associated capacitance, respectively. R_{ct} is the charge transfer resistance and C_{dl} (CPE2) is the associated double-layer capacitance. W_0, which is associated with the low-frequency regions, is Warburg impedance associated with the diffusion resistance R_{diff} [42]. Fig.7 (b) is the equivalent circuit for this impedance spectra. Obviously, the R_{sf} values of the above three samples are comparable, which suggests that the formed SEI film on surface of Si nanoparticle is not related to the amorphous carbon layer of Si particle surface. However, the distinct difference in R_{ct} and R_{diff} can be observed among the three samples. As well known, during the charge-discharge testing, the Si particle experiences a severe expanding and shrinking process, which usually leads to a drop of the electric conduction of Si electrode, and the Li ion transfer in the Si electrode is controlled by the ability of the Si electrode material to transfer the electronic current. The surface amorphous carbon layer can not only suppress the severe expanding and shrinking of Si particle during the charge-discharge testing, but also provide a fast electric conduction network which is benefit for the Li ion intercalation and deintercalation in Si electrode. Thus, those results suggest that the improved cycling property of the Si@C composite is attributed to the improved stable interior structure and electric conduction of Si nanoparticle but not suppressing the formation of SEI films on the surface of the Si surface.

4. CONCLUSION

A Si@C nanocomposite has been prepared successfully by method of in situ polymerization followed by carbonization. The XRD, Raman and HRTEM characterization indicate that the Si@C nanocomposite consists of a silicon core and a thin amorphous carbon layer with thickness of 5 nm. As a promising anode material for lithium ion batteries, after 20 cycles, the Si@C composite exhibits a reversible capacity of 563.2 mAh g^{-1}, and the capacity retention is 88.9%, and good cycle stability, while the conventional Si/C composite and pristine Si exhibit reversible capacity of 193.5 mAh g^{-1} with the capacity retention of merely 27.2% and 129.5 mAh g^{-1} with the capacity retention of only 5.8%, respectively. The improve of cycling property of the Si@C composite is attributed to the improvement of stability and electric conduction of the interior Si nanoparticle, but not suppressing the formation of SEI films on the surface of the Si surface, and therefore ensure the integrity of the structure and the stability of the interface of electrodes. This study also paves a facile and industrial scalable way to prepare core/shell structure with high performance anode materials for lithium-ion batteries.

5. ACKNOWLEDGEMENTS

We gratefully thank the Ministry of Science and Technology (Grant No. 2013CB934000, No. 2011CB935902, No. 2014DFG71590, No. 2010DFA72760, No. 2011CB711202, No. 2013AA050903, No. 2011AA11A257 and No. 2011AA11A254), the China Postdoctoral Science Foundation (Grant No. 2013M530599 and No. 2013M540929), the Tsinghua University Initiative Scientific Research Program (Grant No. 2010THZ08116, No. 2011THZ08139, No. 2011THZ01004 and No. 2012THZ08129) , Beijing Municipal Program (Grant No. YETP0157, No. Z131100003413002 and No. Z131100003413001) , State Key Laboratory of Automotive Safety and Energy (No. ZZ2012-011) and Suzhou (Wujiang) Automotive Research Institute (Project No.2012WJ-A-01).

REFERENCES

[1] J.M. Tarascon, M. Armand, Nature, 414, 359 (2001).

[2] A.S. Arico, P. Bruce, B. Scrosati, J.M. Tarascon, W. Schalkwijk, Nat. Mater., 4, 366 (2005).

[3] M. Armand, J.M. Tarascon, Nature, 451, 652 (2008).
[4] N.S. Ergang, J.C. Lytle, K.T. Lee, S.M. Oh, W.H. Smyrl, A. Stein, Adv. Mater., 18, 1750 (2006).
[5] A.M. Cao, J.S. Hu, H.P. Liang, L.J. Wan, Angew. Chem. Int. Ed., 44, 4391 (2005).
[6] H.S. Zhou, D.L. Li, M. Hibino, I. Honma, Angew. Chem. Int. Ed., 44, 797 (2005).
[7] C. Jiang, E. Hosono, H.S. Zhou, Nano Today, 1, 28 (2006).
[8] G. Armstrong, A.R. Armstrong, P.G. Bruce, P. Reale, B. Scrosati, Adv. Mater., 18, 2597 (2006).
[9] P. Poizot, S. Laruelle, S. Grugeon, L. Dupont, J.M. Tarascon, Nature, 407, 496 (2000).
[10]S. Fang, Y. Tang, X. Tai, L. Yang, K. Tachibana, K. Kamijima, J. Power Sources, 196, 1433 (2011).
[11]S.C. Nam, Y.S. Yoon, K.S. Yun et al, J. Electrochem. Soc., 148 (3), A220 (2001).
[12]Y. Idota, T. Kubota, A. Matsufuji, Y. Maekawa, T. Miyasaka, Science, 276, 1395 (1997).
[13]Y.N. Li, S.L. Zhao, Q.Z. Qin, J. Power Sources, 114, 113 (2003).
[14]Y. Cui, Z. Zhong, D. Wang, W.U. Wang, C.M. Lieber, Nano. Lett., 3, 149 (2003).
[15]L.F. Cui, Y. Yang, C.M. Hsu, Y. Cui, Nano. Lett., 9, 3370 (2009).
[16]Z.S. Wen, J. Yang, B.F. Wang, K. Wang, Y. Liu, Electrochem. Commun., 5, 165 (2003).
[17]K.L. Lee, J.Y. Jung, S.W. Lee, H.S. Moon, J.W. Park, J. Power Sources, 129, 270 (2004).
[18]J.O. Besenhard, J. Yang, M. Winter, J. Power Sources, 68, 87 (1997).
[19]M.W. Verbrugge, Y.T. Cheng, Electrochem. Soc. Trans., 13, 127 (2008).
[20]H. Wu, Y. Cui, Nano. Today, 7, 414 (2012).
[21]M.W. Verbrugge, Y.T. Cheng, J. Electrochem. Soc., 156, A927 (2009).
[22]A.R. Kamali, D.J. Fray, J. New Mater. Electrochem. Systems, 13, 147 (2010).
[23]W.J. Zhang, J. Power Sources, 196, 13 (2011).
[24]H. Li, X. Huang, L. Chen, Z. Wu, Y. Liang, Electrochem. Solid-State Lett., 2, 547 (1999).
[25]J. Graetz, C.C. Ahn, R. Yazami, B. Fultz, Electrochem. Solid-State Lett., 6, A194 (2003).
[26]J. Shu, H. Li, R. Yang, Y. Shi, X. Huang, Electrochem. Commun.,8, 51 (2006).
[27]T. Jiang, S.C. Zhang, X.P. Qiu, W.T. Zhu, L.Q. Chen, Electrochem. Commun., 9, 930 (2007).
[28]L.F. Cui, R. Ruffo, C.K. Chan, H. Peng, Y. Cui, Nano. Lett., 9, 491 (2009).
[29]Y. Yao, M.T. McDowell, I. Ryu, H. Wu, N. Liu, L.B. Hu, W.D. Nix, Y. Cui, Nano. Lett., 11, 2949 (2011).
[30]T. Song, J. Xia, J.H. lee et al., Nano. Lett., 10, 1710 (2010).
[31]Z.B. Zhou, Y.H. Xu, M. Hojamberdiev, W.G. Liu, J. Wang, J. Alloys and Compounds, 507, 309 (2010).
[32]Q. Si, K. Hanai, T. Ichikawa, A. Hirano, N. Imanishi, Y. Takeda, O. Yamamoto, J. Power Sources, 195, 1720 (2010).
[33]S.H. Ng, J. Wang, D. Wexler, K. Konstantinov, Z.P. Guo, H.K. Liu, Chem. Int. Ed., 45, 6896 (2006).
[34]W.R. Liu, J.H. Wang, H.C. Wu, D.T. Shieh, M.H. Yang and N.L. Wu, Electrochem. Soc., 152, A1719 (2005).
[35]M.M. Titirici, A. Thomas, M. Antonietti, Adv. Funct. Mater, 17, 1010 (2007).
[36]J. Yang, B.F. Wang, K. Wang, Y. Liu, J.Y. Xie and Z.S. Wen, Electrochem. Solid-State Lett., 6, A154 (2003).
[37]A.M. Wilson, J.R. Dahn, J. Electrochem. Soc., 142, 326 (1995).
[38]T. Umeno, K. Fukuda, H. Wang, N. Dimov, T. Iwao, M. Yoshio, Chem. Lett., 1186 (2001).
[39]G.X. Wang, J.H. Ahn, Janeyao, Electrochem. Commun., 6, 689 (2004).
[40]A.C. Ferrari, J. Robertson, Phys. Rev. B, 61, 14095 (2000).
[41]P.F. Gao, J.W. Fu, J. Yang, R.G. Lv, J.L. Wang, Y. Nuli, X.Z. Tang, Phys. Chem. Chem. Phys., 11, 11101 (2009).
[42]S.L. Chou, J.Z. Wang, M. Choucair, H.K. Liu, J.A. Stride, S.X. Dou, Electrochem. Commun., 12, 1303 (2010).